Control Circuit Design for Wheel-Leg Hybrid Robot

Mengmeng Luo[1], Xiong Wang[1,*], Jing Zhang[1], Baoliang Wang[2], Fan Li[1]
[1]*School of Energy Engineering, Yulin University, Yulin, Shaanxi, China*
[2]*Shengsheng Environmental Protection Technology Co., Ltd., Yulin, Shaanxi, China*
**Corresponding Author*

Abstract: To meet the stringent requirements of miniaturization, ease of operation, and integral body deformation for advanced mobile robots, this paper focuses on the customized design of a dedicated control circuit for the YLRobot-III wheel-leg hybrid robot. The STC12C5A60S2 microcontroller is carefully selected as the core control unit, thanks to its high integration and strong compatibility with peripheral components. On this basis, a complete set of auxiliary circuits are elaborately constructed, including stable power supply, reliable reset, high-precision crystal oscillator, high-response servo drive, and efficient DC motor drive modules. Specifically, the servo rotation angle is accurately controlled by adjusting the high-level duration of the PWM signal, while the DC motor speed is flexibly regulated by modifying the PWM duty cycle. Comprehensive simulation analyses and practical experimental verifications are carried out, which confirm the excellent effectiveness and high precision of the proposed control methods, demonstrating the robot's reliable capability to realize precise joint rotation and stable wheel movement. This further provides robust technical support for the motion control of wheel-leg hybrid robots.

Keywords: Leg-rotor Hybrid Robot; Control Circuit; Servo Motor; DC Motor

1. Introduction

Nowadays, robot technology is developing rapidly, and the application fields of mobile robots are constantly expanding. From industrial production to scientific exploration, from military reconnaissance to daily life services, their importance is becoming increasingly prominent [1]. As a type of mobile robot integrating wheeled and legged structures, wheel-leg hybrid robots have attracted widespread attention in recent years [2].

At present, certain progress has been made in the research of wheel-leg hybrid robots at home and abroad. Harbin Institute of Technology released the WLR-3P robot in 2022. This robot has a hydraulically driven wheel-leg hybrid structure, with independent degrees of freedom at the hip joint, knee joint, and driving wheel, thus combining the advantages of wheeled and legged robots. However, the hydraulic system is relatively complex, which increases the volume, weight, and cost of the robot, and does not conform to the current mainstream direction [3-4].

GAC Group launched the GoMate robot in 2024. The robot has 38 degrees of freedom in total, adopting a variable wheel-foot mobile structure that integrates two modes: four-wheel-foot and two-wheel-foot, driven by servo motors. GoMate incorporates a visual autonomous driving algorithm, can respond to complex human voice commands, and simultaneously has the advantages of efficient wheeled movement and flexible legged obstacle surmounting. However, due to its integration of various advanced and complex technologies, it has high professional requirements for operation and maintenance, which to a certain extent limits its application in many scenarios where the professional quality of operators is not high [5].

A spin-off company from ETH Zurich developed the Swiss-Mile robot in 2024. The robot has 8 degrees of freedom, with 2 degrees of freedom allocated to each leg, set at the hip joint and knee joint respectively. The robot is driven by servo motors. In the wheeled motion mode, the servo motors can quickly and accurately control the rotation of the wheels to assist the robot in moving forward rapidly. When switching to the legged motion mode, the servo motors can control the leg joints to cross various complex obstacles. However, the number of degrees of freedom of the robot's legs is limited, and its mechanical structure cannot undergo significant transformation, which affects its application scenarios [6].

To promote the application of wheel-leg hybrid robots in more scenarios, especially to meet the requirements of miniaturization, ease of operation, and overall deformation, this paper proposes a new type of wheel-leg hybrid robot YLRobot-III. On this basis, the control circuit and control method are studied to ensure the full performance of the robot and provide a reference for the circuit design of other robots.

2. YLRobot-III

As shown in Figure 1, the YLRobot-III robot features dual movement modes: a humanoid form when walking and a vehicle-like configuration when driving, enabling full-body transformation.

The foot structure is shown in Figure 1(a). The two symmetrical mechanical legs each have three degrees of freedom, comprising three leg joints: hip joint, knee joint, and ankle joint. Each joint is controlled by one actuator, totaling six actuators. By rotating the actuators to specific values, the joint angles are adjusted to achieve foot movement. A drive wheel is mounted on the top, while auxiliary driven wheels are installed on the foot.

When the robot transitions from foot-based movement to wheeled movement, all six actuators must drive their respective joints to participate in the motion. The initial state is shown in Figure 1(a), where the hip and knee joints rotate, deforming the robot into a vehicle shape with the top touching the ground. Subsequently, the ankle joints rotate to make the auxiliary driven wheels contact the ground, as illustrated in Figure 1(b), thereby completing the mode transition of the robot.

In wheeled mode, the robot moves rapidly using wheels. The wheeled structure consists of two wheel assemblies, each containing one drive wheel and one auxiliary driven wheel. Two DC motors control the two drive wheels.

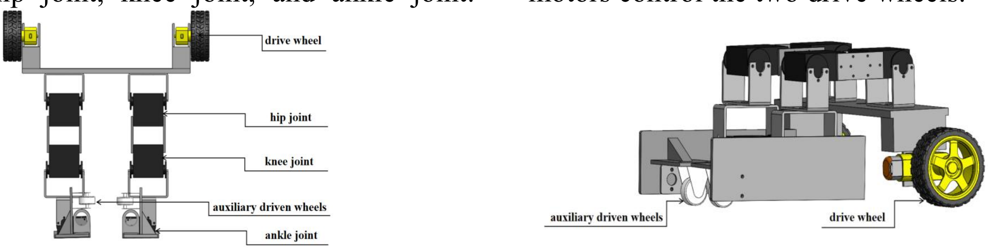

(a) Foot Structure **(b) Wheeled Mode**

Figure 1. YLRobot-III

3. Control Circuit and Control Method

3.1 Control Circuit

Clearly, controlling the robot's movement requires managing both the servo and DC motor. The STC12C5A60S2 microcontroller was selected as the controller for the YLRobot-III [7], with its 40 I/O pins fully meeting the control requirements.

As shown in Figure 2, the drive servos for the robot's left leg (hip, knee, and ankle joints) are designated as 1, 2, and 3, respectively, while those for the right leg are 4, 5, and 6. The drive wheels are equipped with DC motors, specifically DC speed reducing motors numbered 1 and 2.

The microcontroller controls the steering gear and DC motor by PWM, and realizes the foot movement, wheel movement and mode change.

3.1.1 Controller circuit

To enable the microcontroller to operate, the power supply, reset, and crystal oscillator circuits are designed as shown in Figure 3. The 5V power supply is connected to the VCC and GND pins, providing stable voltage to the controller and ensuring proper operation of all circuit components. The power-on reset is achieved through the RST pin using a 10μF capacitor and 10kΩ resistor, restoring the microcontroller to its initial state during startup or abnormal conditions. The microcontroller receives a stable clock signal from XTAL1 and XTAL2, which utilize a 12MHz crystal oscillator paired with 30pF capacitors, ensuring precise clock speed and timing accuracy for the controller.

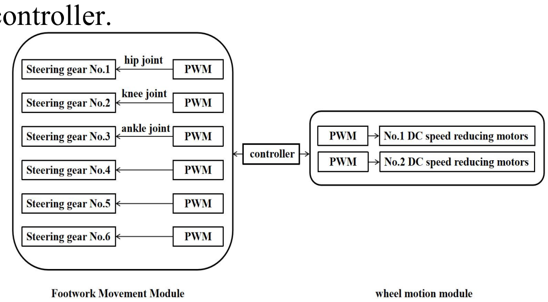

Figure 2. Control Circuit

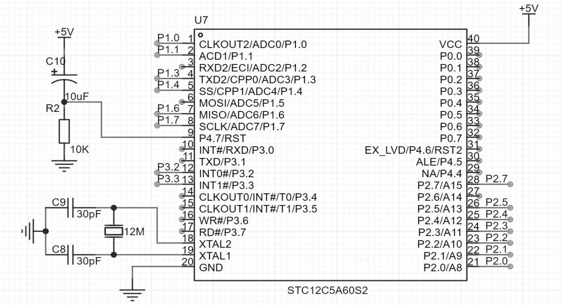

Figure 3. Controller Circuit

3.1.2 Steering gear control circuit

The steering gear employs the Hayward LX-824HV model, featuring a 7.4V power supply and 0-180° rotation range. It includes three ports: positive/negative power terminals and a data input port. As shown in Figure 4, the steering gears numbered 1-6 are connected to the microcontroller's P2.0-P2.5 pins. By sending precise PWM signals to these pins, the microcontroller controls each gear's rotation angle and speed, enabling the robot to perform legged movements and mode transitions.

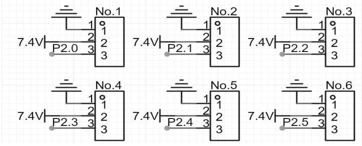

Figure 4. Steering Gear Control Circuit

3.1.3 DC motor control circuit

The system employs an MF7997 DC motor with a no-load speed of 1000 r/min at 5V. The L298N driver is used to control the motor. As shown in Figure 5, 7.4V serves as the drive voltage, while 5V provides logic power. Two 100μF capacitors are connected in parallel at 5V, and a 100μF capacitor with a 0.1μF capacitor in parallel at 7.4V for filtering. An array of eight freewheeling diodes provides a discharge path for back EMF during power interruption or commutation. OUT1-OUT4 interfaces with the two DC motors. The microcontroller connects to the L298N via port P1, driving the H-bridge with PWM signals to control the motors, enabling the robot's wheel-based movements including forward/backward and left/right turns.

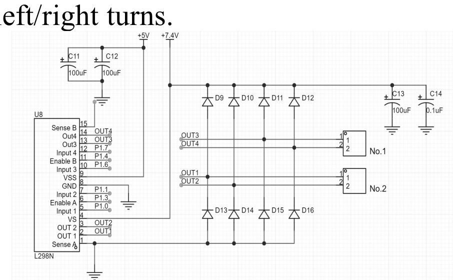

Figure 5. DC Motor Control Circuit

3.2 Control Method

3.2.1 Steering gear control

As previously discussed, robots utilize PWM to control servo motors. The core of PWM control lies in the time width between its rising and falling edges. By adjusting the proportion of high-level duration within the PWM clock cycle, the system can regulate the servo motor's rotation angle and speed [8].

The STC12C5A60S2 is an 8-bit microcontroller with a data resolution of 256. Based on the operational parameters of the 180 servo motor, the data is divided into 250 segments. The high-level duration of the 180 signal ranges from 0.5 to 2.5 milliseconds, with a pulse width of 2 milliseconds.

The control precision of the steering gear is shown in Equation (1).

$$\frac{180^\circ}{250} = 0.72^\circ \quad (1)$$

The control precision of PWM is given by Equation (2).

$$\frac{2ms}{250} = 8\mu s \quad (2)$$

The servo motor requires a minimum PWM high-level duration of 0.5ms, with the low-level width determining its rotation speed. Assuming N as the number of divisions, the motor rotates through 0.72 degrees per division (0.72°×N), corresponding to a PWM high-level width of 0.5ms plus 8μs multiplied by N [9].The PWM waveform of the servo motor is illustrated in Figure 6.

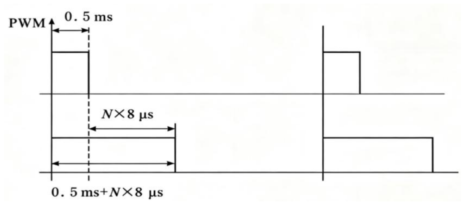

Figure 6. PWM Waveform Diagram of Servo

3.2.2 DC motor control

DC motors also utilize PWM control [10]. The control mechanism operates by switching the power supply at a fixed frequency, adjusting the duration of on-off cycles within a given period to modify the duty cycle D of the armature voltage. This adjustment enables variation in the average voltage level, thereby achieving different motor average speeds Va for speed regulation.

T denotes the period, with t_1 being the duration of power supply activation within one cycle. The duty cycle is given by Equation (3).

$$D = \frac{t_1}{T} \quad (3)$$

V denotes the rotational speed of the motor under full-voltage drive. The average speed of the motor, V_a is approximately given by Equation (4).

$$V_a = V \times D \quad (4)$$

4. Simulation and Experimental Verification

4.1 Simulation

The effectiveness and accuracy of the circuit of the servo and DC motor and the control method based on PWM are verified by simulation.

4.1.1 Servo control simulation

The target steering angle is set to 90 degrees, corresponding to a PWM high-level duration of 1.5ms. The program is programmed to control the steering mechanism and run the simulation. For future experimental results, the No.3 and No.6 steering motors of the ankle joint are selected as control targets. As shown in Figure 7, the steering motor rotates from the initial angle of 0 degrees and stabilizes at 90 degrees. This aligns with the theoretical target angle, demonstrating the effectiveness of PWM control in steering angle simulation.

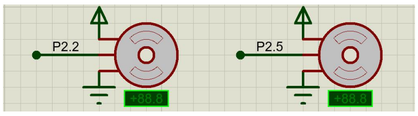

(a) Initial position of the rudder 0

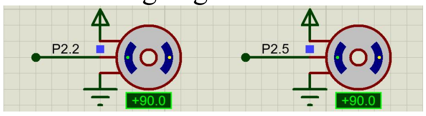

(b) The steering gear reaches position 90.

Figure 7. Servo Control Simulation Diagram

4.1.2 Simulation of DC motor control

A simulation program was developed to control the DC motor. As shown in Figure 8(a), the motor speed reached 988 rpm the simulation environment. After significantly reducing the duty cycle, the speed dropped to 462 rpm. This demonstrates that the control of the DC motor is controllable under the simulation conditions.

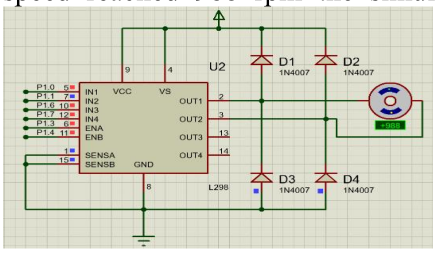

(a) The DC motor operates at a speed of 988 rpm

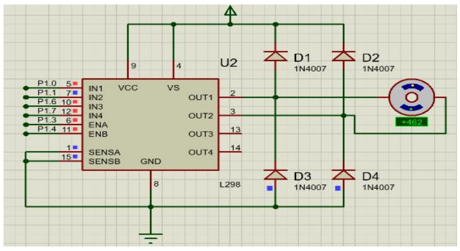

(b) The DC motor operates at a speed of 462 rpm

Figure 8. DC Motor Control Simulation Diagram

4.2 Experimental Verification

4.2.1 Verification of the steering gear control experiment

The YLRobot-III was physically tested by driving its No.3 and No.6 servos to activate the two ankle joints. Starting from an initial angle of 0 degrees, the robot rotated steadily to 90 degrees, allowing the auxiliary driven wheel to make smooth contact with the ground. As shown in Figure 9, the experimental results confirm that the robot successfully performs servo control.

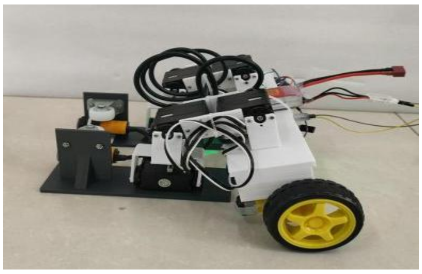

(a) Physical images of the 3rd and 6th steering gears at position 0°

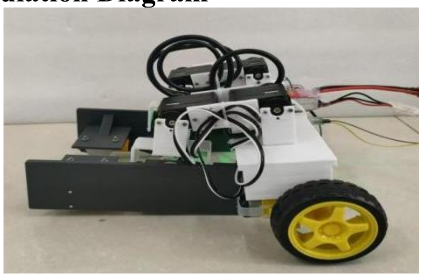

(b) Physical image of the 3rd and 6th steering gears at position 90°

Figure 9. Test Verification Diagram of Servo

4.2.2 Verification of DC motor control experiment

When both motors 1 and 2 are running in forward rotation with a duty cycle of 1, the measured rotational speed is 980 rpm. The duty cycle is set to 0.015, and the timing duration is 0.2 minutes. The wheel diameter d is 65 mm.

The total distance L of the theoretical motion is approximately given by Equation (5).

$$L = VD \times 0.2 \times \pi d = 600\text{mm} \quad (5)$$

As shown in Figure 10, actual measurements indicate the robot traveled approximately

550mm forward within 0.2 minutes, which is lower than the theoretical calculation. This discrepancy occurs because the actual rotational speed is lower than the value derived from the duty cycle calculation.

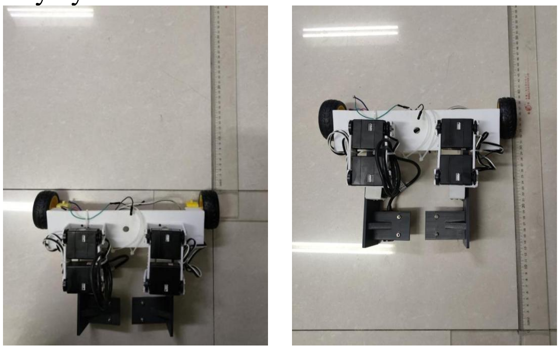

(a) Initial position image **(b) Position image after 0.2 minutes**

Figure 10. Experimental Verification of DC Motor

The experimental results show that the robot can control the steering gear and DC motor rotation angle, and achieve the expected goal accurately, which further verifies that the motor control method can effectively control the robot.

5. Conclusion

Simulation and experimental results demonstrate that the control circuit and corresponding control method designed for the legged bipedal robot in this paper can effectively manage both the servo motor and DC motor, enabling precise motion control. The proposed circuit and method exhibit universal applicability, providing a reference for controlling similar types of robots. Subsequently, we will conduct further research on the motion performance of legged bipedal robots based on the control of servo motors and DC motors.

Acknowledgments

This work was supported by the Yulin Municipal Bureau of Science and Technology Industry-University-Research Project (2023-CXY-141); Shaanxi Provincial Department of Education Scientific Research Program Project (23JP201); Yulin University Horizontal Research Project (H2024060240).

References

[1] Li Jinfu, Yu Ze, Lian Binbin. Design and Analysis of a Multimodal Wheel-Legged Mobile Robot. Journal of Tianjin University, 2025, 58(01): 12-23.
[2] Yang Bowen, Gou Kunyi, Yang Wanli, et al. Structural Design and Kinematics Simulation of Wheel-leg Robot. Robot Technology and Application, 2025, (04): 21-26.
[3] Liu Chao, Tan Xicen, Yao Yan'an, et al. Design and Analysis of a Novel Deformable Wheel-legged Robot. Journal of Mechanical Engineering, 2022, 58(03): 65-74.
[4] Chen Haoxiang, Weng Zhidan, Yu Yaxin, et al. Research on Hydraulic Legged Robot Joint Drive System Testing Platform. Machinery & Electronics, 2024, 42(07): 57-63, 68.
[5] Mo Shuai, Li Yuhua, Yang Zhenning, et al. Design of brushless server's drive-and-control system for robot joints. Journal of Machine Design, 2023, 40(02): 50-56.
[6] Shi Yusheng, Zhang Minglu, Zhang Xiaojun, et al. Optimization Design and Obstacle Climbing Performance Research of a Transformable Wheel-leg Hybrid Robot. Journal of Mechanical Engineering, 2025, 61(11): 45-56.
[7] Liang Mingliang, Sun Yijie. Design of the Intelligent Robot Based on the STC12C5 A60S2 MCU. Journal of Jixi University, 2012, 12(05): 41-42, 48.
[8] Chen Chaoran, Deng Yong, Huang Dong. Research on Control Accuracy of Robot Servo. Mechanical Engineering & Automation, 2024, (05): 32-34, 37.
[9] Wu Yujun. Single chip microcomputer control technology of multi steering gear. Electronic Test, 2016, (14): 37, 43.
[10]Yin Dongmei. PWM DC Motor Speed Regulation System Based on Single-chip Microcomputer Control. Public Communication of Science & Technology, 2015, 7(24): 155, 157.

